Available online at www.sciencedirect.com
ScienceDirect
Applied Ocean Research 28 (2006) 9–17
Applied Ocean Research
www.elsevier.com/locate/apor

A numerical study of the breaking of modulated waves generated at a wave maker

Andonowati[a,b,*], W.M. Kusumawinahyu[a], E. van Groesen[b]

[a] *Department of Mathematics, Institut Teknologi Bandung, Jl. Ganesha 10, Bandung, Indonesia*
[b] *Department of Applied Mathematics, University of Twente, P.O. Box 217, 7500AE Enschede, The Netherlands*

Received 11 November 2005; accepted 10 May 2006
Available online 21 July 2006

Abstract

This paper is concerned with breaking criteria for generated waves. An input in the form of a time signal is prescribed to a wave maker located at one end of a wave tank as used in hydrodynamic laboratories. The motion of this wave maker produces waves propagating into initially still water in the tank. The spatial evolution of the wave train is referred to as the signaling problem to distinguish from an initial value problem that investigates the temporal evolution of a given initial wave profile. A numerical simulation of the nonlinear propagation of time traces along the tank is investigated to see if breaking occurs and, if so, at which location in the tank. A quantity is proposed as a breaking indicator that is based on a modification of a mean convergence rate of the squared steepness, recently suggested by Song and Banner for the initial value problem. Two classes of waves, namely Benjamin–Feir and bichromatic waves, are considered as influx to the wave maker. A comparison between the signaling problem and the initial value problem for these two classes is presented. The result of the investigations is that, for both classes, the initial steepness can be more extreme in the signaling case than in the case of the initial value problem such that there is no breaking during their evolution. Furthermore, the modified quantity shows the existence of a threshold value for breaking, below which no breaking can occur.

Keywords: Signaling problem; Breaking; Wave generation; Steepness; Benjamin–Feir; Bichromatic

1. Introduction

Investigations on extremely high ocean waves, often called freak waves, have been the subject of extensive studies over the past few years due to their potentially hazardous effects on ships, offshore structures and floating objects. Generally speaking, an extreme wave is a very large wave with a wave height H that exceeds the significant wave height H_s by a factor of 2.2 of the measured wave trains (Dean [1]). Of particular interest are extreme waves in the form of wave group structures; these are discussed in several papers, among which insightful investigations are presented in Longuet-Higgins [2], Phillips [3], and Donelan [4]. The dynamics of such waves is often described as a nonlinear self-focusing phenomenon resulting in very steep waves of high amplitude arising intermittently within the wave group structures (Henderson [5], Dysthe [6]). These self-focusing effects are often attributed to the modulation instability of Benjamin–Feir (BF) [7] when the modulation of a monochromatic wave is long enough and lies within the region of BF instability. Related to the steepness of the waves, breaking may occur during the wave evolution. In Donelan [4], Holthuijsen [8] and Osborne [9] among others, investigations are presented on extreme waves linked to wave breaking for wave group structures. In a recent paper by Onorato [10], the generation of freak waves in a random ocean wave train is investigated using a so-called time-like NLS equation characterized by the JONSWAP power spectrum. The investigation by Onorato [10] differs from this research, where we deal with *deterministically generated* extreme waves.

This research is motivated by the requirement of hydrodynamics laboratories to generate extreme waves for testing ships in steep, large-amplitude wave fields. Because of physical and technical limitations, direct generation of such extreme waves

* Corresponding address: Institut Teknologi Bandung, Centre for Mathematical Modelling and Simulation, Jl. Ganesha 10, 40132 Bandung, Indonesia. Fax: +62 22 2508126.
E-mail addresses: aantrav@attglobal.net, andonowatia@math.utwente.nl (Andonowati).

0141-1187/$ - see front matter © 2006 Elsevier Ltd. All rights reserved.
doi:10.1016/j.apor.2006.05.001

by the wave maker is not possible. But the nonlinear effects will help: a suitable input signal given to the wave maker will deform and the amplitude increases while propagating in the tank. Exploiting this fact, given the position in the wave tank where extreme waves have to be produced for testing ships, it is necessary to predict the required wave-maker motion. In this generation process, it is important that the generated waves do not break during the downstream propagation toward the test position. For this purpose, finding criteria that determine if breaking will occur for propagating waves is important. This type of problem will be referred to as a signaling problem.

Observations on the onset of wave breaking have been conducted widely, see e.g. Song and Banner [11], Banner and Tian [12], Griffin et al. [13], Melville [14], Tulin and Li [15], Rapp and Melville [16], and Kway et al. [17] among others. All these papers deal with the time-dependent evolution from given initial wave fields that lead to wave breaking later. In a specialized study on wave breaking, Song and Banner [11,12] investigate the evolution of a quantity that can be referred to as the maximum squared steepness. Song and Banner proposed a predictor for wave breaking that is based on a quantity $\mu(t)$ that is defined by

$$\mu(t) = \max_x \left[\frac{E(x,t)}{\rho_w g} k^2(x,t) \right], \tag{1}$$

where $E(x,t)$ is the depth integrated energy; for a layer of fluid in irrotational motion with potential ϕ and wave elevation $\eta(x,t)$, E is given explicitly by

$$E(x,t) = \int_{-h}^{\eta(x,t)} \frac{1}{2}\rho_w(\phi_x^2(x,z,t) + \phi_z^2(x,z,t))\mathrm{d}z + \frac{1}{2}\rho_w g \eta^2(x,t) \tag{2}$$

where ρ_w, g and h are the water mass density, the gravitational acceleration and the still water depth, respectively. The local wave number $k(x,t)$ is computed in [11] using a *Hilbert* transformation, followed by low-pass filtering as a refinement in [12].

They considered the initial value problem for three classes of initial wave groups, among which are a monochromatic wave perturbed by a small symmetric sideband, referred to here as the Benjamin–Feir instability case, and one case of bichromatic waves. The first class of wave groups, the Benjamin–Feir instability case, has an initial profile of the form

$$\eta(t=0,x) = a_0\cos(k_0 x) + \epsilon a_0 \cos\left(\frac{N+1}{N}k_0 x - \theta\right) + \epsilon a_0 \cos\left(\frac{N-1}{N}k_0 x - \theta\right). \tag{3}$$

Here, k_0 is the wave number of the uniform wave train, k_0/N is the wave number of the long modulation perturbations, and N can be interpreted as the number of waves in one modulation. In the following, we will follow that paper and consider $k_0 = 1, \epsilon = 0.1, 3 \le N \le 10, \theta = \pi/4$. The second class considered, the bichromatic case, has an initial profile of the form

$$\eta(t=0,x) = a_0\cos(k_0 x) + a_0 \cos\left(\frac{N+1}{N}k_0 x - \frac{\pi}{18}\right), \tag{4}$$

where $k_0 = 1$, and N is the same as in the first case.

In both cases, the time evolution of these initial profiles is obtained in [11] with a Dold and Peregrine (DP) code based on a boundary integral for a fully nonlinear, two-dimensional, inviscid model of free-surface gravity water waves in a periodic domain (Dold [18]). For these classes, the existence of a common threshold value δ_{th} as a breaking criterion is found. This value, defined as $\delta_{\mathrm{th}} = \frac{1}{\omega_0}\frac{\partial\langle\mu(t)\rangle}{\partial t}$, is related to the mean convergence rate of this squared steepness, where $\langle\mu(t)\rangle$ is an average of $\mu(t)$.

The aim of this paper is to investigate the propagation of generated wave fields and to study in which cases the wave field will or will not break. Further, in case of breaking, we are interested in the location within the wave tank where the waves start to break. To achieve our aims, we consider at every position the maximum over time of the product of energy and squared wave number, which is akin to the squared steepness. Here, we have to adjust the parameters of breaking defined in [11] for μ and δ.

Data for this investigation are generated by using a numerical wave tank HUBRIS developed by Westhuis [19–21]. The code has been tested extensively against experimental data at the Maritime Research Institute Netherlands (MARIN). Among these tests are cases of the generation of extreme and unstable bichromatic wave groups [22,23]. In these tests, a large number of comparisons are made between experiments and numerical simulations. Although the code cannot describe the phenomena of breaking itself, it detects the onset of breaking. In all test cases, the breaking in the experiments corresponds to breaking in the simulations. Furthermore, the performance of the code with respect to beaches and reflections has been reported in [24].

The organization of this paper is as follows. In the next section, we briefly describe the generation of data used in this paper. Results on the initial wave steepness at the wave maker, the wave breaking indicator, as well as some analysis on these results, are presented in Section 3. A comparison with experiments of the initial steepness for breaking waves is also presented in this section. In the last section, we draw some concluding remarks.

2. Generation of data

In order to generate the time signal at the wave maker and calculate its spatial evolution, a numerical code called HUBRIS is used. The code is a numerical wave tank based on a fully nonlinear free-surface wave model with a wave generator on one side and an absorbing beach on the other [19–21]. This model is Laplace's equation for the potential velocity in the interior, together with the fully nonlinear kinematic and dynamic boundary conditions on the free surface. The code is based on the finite-element method (FEM) which is suitable for the wave tank considered. Such a realistic wave tank is typically

200 m long and 5 m deep. Since the length is significantly larger than the depth, the resulting stiffness matrix is banded and symmetric with a small number of bands, depending on the number of grid points used for the water depth.

HUBRIS provides several options for the wave generation. The option used in this paper is by generating a generalized numerical velocity using a combined flux–displacement wave maker. The idea here is to allow arbitrary correlation between the prescribed velocity on the inflow boundary and the actual displacement of the boundary. This correlation in HUBRIS is parameterized by a parameter σ. For $\sigma = 1$, the wave-maker boundary produces the numerical influx, where the normal velocity along the boundary is provided according to the virtual motion of the wave maker. In this case, the boundary influx can be seen as a model for a complicated non-uniform pump system. For other values of σ, the wave-maker boundary is a mix of flap/piston motion and influx. For the purpose of increasing the stability of the simulation, we chose the option with $\sigma = 1$ for the investigation in this paper. Second-order steering, to avoid free waves, as discussed in [23], is applied.

In the following, to avoid interference with possibly small reflected waves from the wave absorber, all data are generated for an extended length of the basin to assure that reflection from the wave absorber is negligible.

For the data generation, we set the length of the wave tank, excluding the additional length for wave absorption, to be $L = 200$ m, the water depth as $h = 5$ m, and the maximum time of the simulation as $T_s = 300$ s. The resolution in spatial variables is taken to be $\Delta x = 0.2$ m and, for time, $\Delta t = 0.1$ s. In the cases of our interest, the maximum observation interval T_s is at least twice as long as the travel time from the wave maker to the absorber. In all the generated data, all quantities related to the wave-breaking indicator are calculated over a retarded time interval from $T_0 = t_0 + L/V_g$ to T_s. Here, V_g is the linear wave group velocity at the center frequency of the wave. The time t_0 is added so that entrance effects have taken place already. This is solely to get a good record for measuring the breaking indicators and to get an accurate dependence on the input at the wave maker. It should be noted that the time interval on which we decide about the breaking starts at $t = 0$.

The interest here is to find the largest value of the initial steepness at the wave maker so that the resulting waves propagating into the tank do not break. Although the code cannot calculate overturning waves, breaking is indicated by blow-up of the calculation; as stated previously, comparison with experiments has shown that this corresponds well with breaking in reality. All generated data are presented in laboratory dimensions [m, kg, s].

For the BF case, the signal at the wave maker is of the form

$$\begin{aligned}\eta(x=0,t) &= a_0\cos\bar{\omega}t + \epsilon a_0\cos\omega_+ t + \epsilon a_0\cos\omega_- t,\\ &= a_0(1+2\epsilon\cos\nu t)\cos\bar{\omega}t\end{aligned}$$

where parameters are adjusted to agree with those in [11], i.e. $\omega_\pm = \Omega(\frac{N\pm1}{N}k_0)$, $\bar{\omega} = \frac{\omega_+ + \omega_-}{2}$, $\epsilon = 0.1$, $\nu = \frac{\omega_+ - \omega_-}{2}$, and $k_0 = 1$. Here we use the dispersion relation for linear waves, $\omega = \Omega(k) = \sqrt{gk\tanh(kh)}$, to relate the frequency ω and the wave number k for a given water depth h and gravitational acceleration g. In this BF case, at the wave maker the monochromatic signal $\cos\bar{\omega}t$ with a period $T_{\text{wave}} = 2\pi/\bar{\omega}$ is modulated by an envelope $a_0(1+2\epsilon\cos\nu t)$ with a large period $T_{\text{env}} = 2\pi/\nu$.

To illustrate the meaning of the parameter N in the BF case, let us take $N = 5$. For this case, the monochromatic frequency $\bar{\omega} = 3.1160$/s corresponds to the period of the signal $T_{\text{wave}} \approx 2.0164$ s, while the modulation frequency $\nu = 0.3150$/s corresponds to the period for the envelope $T_{\text{env}} = 19.9466$ s. Thus at the wave maker, for $N = 5$, in one envelope of the time signal there are approximately ten monochromatic waves while the corresponding spatial envelope contains five waves. This signal at the wave maker, $\eta(x = 0, t)$ for $N = 5$, is plotted in Fig. 1. From the dispersion relation, it can easily be shown that the number of monochomatic waves in one envelope of this BF time signal is approximately twice as many as the number of waves in its spatial envelope; $\bar{\omega} \approx 2N\nu$ while $k_0 = N\kappa$, where $\kappa = (\frac{N+1}{N}k_0 - \frac{N-1}{N}k_0)/2$. For $N = 5$, the wavelength of the spatial envelope is $\lambda = 2\pi/\kappa$ m $= 10\pi$ m.

We also calculated the *initial steepness*, defined as $s_0 = a_0k_0$. In Table 1, we summarize the different parameters used to generate various signals.

For the bichromatic case, the signal at the wave maker is

$$\begin{aligned}\eta(x=0,t) &= a_0\cos(\omega_0 t) + a_0\cos(\omega_+ t),\\ &= (2a_0\cos\nu_1 t)\cos\bar{\omega}_1 t\end{aligned}$$

where $\omega_+ = \Omega(\frac{N+1}{N}k_0)$, $\omega_0 = \Omega(k_0)$, $\bar{\omega} = \frac{\omega_+ + \omega_0}{2}$, $\nu_1 = \frac{\omega_+ - \omega_0}{2}$, and $k_0 = 1$ are taken as in [11]. Here, the monochromatic signal $\cos\bar{\omega}t$ with period $T_{\text{wave}} = 2\pi/\bar{\omega}$ is modulated by an envelope $2a_0\cos\nu_1 t$ with a large period $T_{\text{env}} = 2\pi/\nu_1$. The parameters used in the signal generation for this case are shown in Table 2.

To compare with the BF case, let us consider the bichromatic signal at the wave maker for $N = 5$. The monochromatic frequency for this case is $\bar{\omega} = (\omega_0 + \omega_+)/2 = 3.2815$/s, while the modulation frequency is $\nu_1 = 0.1495$/s. Thus the period for the signal is $T_{\text{wave}} \approx 1.9147$ s and the period for the envelope is $T_{\text{env}} \approx 42.0280$ s. In the bichromatic case, as illustrated in Fig. 3, one envelope makes two beats, and so for $N = 5$ there are approximately 10 monochromatic waves in one beat.

3. Results

We now present the results of the calculations as well as an analysis of these results. We divide them into four parts: the initial steepness for breaking and a comparison with experiments, the wave-breaking indicator, the wave-breaking criterion for the signaling problem, and a comparison of the breaking parameter for the initial value problem and the signaling problem.

3.1. Initial steepness at the wave maker

In what follows, we show some results of wave signals at various positions. In Figs. 1 and 2, we show signals for BF with

Table 1
Parameters used in the Benjamin–Feir signaling problem (BF), and the corresponding parameters for the initial value problem (IVP) used in Song and Banner

Case	Parameter						Related quantities for IVP			
R/B	N	a_0	$\bar{\omega}$	ω_-	ω_+	ν	s_0	k_0	k_-	k_+
R	3	0.166	3.0865	2.557	3.616	0.5295	0.166	1	0.666	1.333
B	3	0.167	3.0865	2.557	3.616	0.5295	0.167	1	0.666	1.333
R	5	0.140	3.1160	2.801	3.431	0.3150	0.140	1	0.800	1.200
B	5	0.141	3.1160	2.801	3.431	0.3150	0.141	1	0.800	1.200
R	7	0.133	3.1235	2.899	3.348	0.2245	0.133	1	0.857	1.143
B	7	0.134	3.1235	2.899	3.348	0.2245	0.134	1	0.857	1.143
R	8	0.136	3.1255	2.929	3.322	0.1965	0.136	1	0.875	1.125
B	8	0.137	3.1255	2.929	3.322	0.1965	0.137	1	0.875	1.125
R	10	0.140	3.1280	2.971	3.285	0.1570	0.140	1	0.900	1.100
B	10	0.141	3.1280	2.971	3.285	0.1570	0.141	1	0.900	1.100

The BF signal at the wave maker contains the frequency of the monochromatic carrier $\bar{\omega}$ and two side-band frequencies ω_+ and ω_-. For each N, a wave group is obtained: a monochromatic $\cos(\bar{\omega}t)$ modulated by an envelope $a_0 + 2\epsilon a_0 \cos(\nu t)$. Here, a_0 is the amplitude of the monochromatic $\cos(\bar{\omega}t)$ and ϵa_0, with small ϵ, is the amplitude of each side-band wave. The envelope of the time signal at the wave maker contains approximately $2N$ of the monochromatic carriers, while the spatial envelope contains N monochromatic carrier waves.

Table 2
Parameters used in the signaling problem for the bichromatic case and the corresponding parameters for the initial value problem (IVP) used in Song and Banner

Case	Parameter					Related quantities for IVP		
R/B	N	a_0	ω_0	ω_+	ν_1	s_0	k_0	k_+
R	3	0.092	3.132	3.616	0.2422	0.092	1	1.333
B	3	0.093	3.132	3.616	0.2422	0.093	1	1.333
R	5	0.084	3.132	3.431	0.1495	0.084	1	1.200
B	5	0.085	3.132	3.431	0.1495	0.085	1	1.200
R	7	0.080	3.132	3.348	0.1080	0.080	1	1.143
B	7	0.081	3.132	3.348	0.1080	0.081	1	1.143
R	8	0.077	3.132	3.322	0.0950	0.077	1	1.125
B	8	0.078	3.132	3.322	0.0950	0.078	1	1.125
R	10	0.072	3.132	3.285	0.0765	0.072	1	1.100
B	10	0.073	3.132	3.285	0.0765	0.073	1	1.100

We consider bichromatic signals at the wave maker containing two frequencies ω_+ and ω_0 that are close to each other. The monochromatic $\cos(\bar{\omega}t)$ is modulated by the envelope $2a\cos(\nu_1 t)$, where $\bar{\omega} = (\omega_+ + \omega_0)/2$ and $\nu_1 = (\omega_+ - \omega_0)/2$. Different from the BF signals, both monochromatic components have the same amplitude.

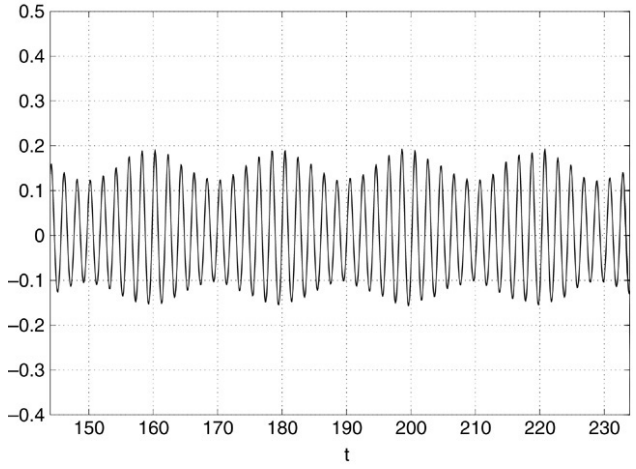

Fig. 1. Benjamin–Feir signal at the wave maker for $N = 5$: the monochromatic frequency $\bar{\omega} = 3.1160$ corresponds to the period of the carrier signal $T_{\text{wave}} \approx 2.0164$ s, while the modulation frequency $\nu = 0.3150$ corresponds to the period for the envelope $T_{\text{env}} = 19.9466$ s. Thus at the wave maker, for $N = 5$, in one envelope of the time signal there are approximately 10 monochromatic carrier waves. The corresponding spatial envelope of the initial value problem contains fives waves.

$N = 5$ for a recurrent (non-breaking) case at different locations, namely at the wave maker $x = 0$ and at $x = x_{\max}$. Here $x_{\max}$ is defined as follows. Let $\alpha(x)$ be the so-called maximum temporal amplitude (MTA) of a generated signal, defined as in Andonowati and Van Groesen [25] as the maximum over time of the signal at each given location along the wave tank; $\alpha(x) = \max_t \eta(x,t)$. We then take $x_{\max}$ to be the position where MTA achieves the maximum value. Through this concept of MTA, the position where the largest wave elevation occurs within the wave tank can be readily deduced. Furthermore, the amplification factor, that is, the ratio between the elevation of the signal at the wave maker and the largest elevation of the signal along the tank, can be obtained from $\alpha(x_{\max})/\alpha(0)$. For the case of the BF signal with $N = 5$, this amplification factor is approximately 2.5. Figs. 1 and 2 show how the BF signal deforms from its original signal produced at the wave maker.

Figs. 3 and 4 show samples of signals for bichromatics for $N = 5$ for a recurrent case at the wave maker, $x = 0$, and at $x = x_{\max}$. Observe that there are approximately 10 individual waves in one beat. Comparing these two signals at the wave maker and at its largest elevation, we deduce that the amplification factor is approximately 2.

The major results about breaking are summarized in Table 3. Both for BF and for bichromatics, the results of Song and Banner (IVP) and the results of our calculations (signaling problem) are presented. In each case and for each N, the given value of the initial steepness, s_0, is the threshold value for recurrence (R) or breaking (B). The term recurrence refers to the temporal recurrence; for a given position in the tank, we observe similar patterns in the signals at least twice. Here the time interval of the observation is taken as at least twice as long as the travel time from the wave maker to the absorber. The threshold value is the limiting value of s_0 at the wavemaker above which breaking occurs within that tank.

Table 3
Comparison of the initial steepness for the initial value problem (IVP) and the signal steepness at the wave maker for the signaling problem for the Benjamin–Feir and bichromatic cases

N	R/B	Benjamin–Feir case			Bichromatics case		
		s_0 for IVP	s_0 for SP	x_{max}/x_{break}	s_0 for IVP	s_0 for SP	x_{max}/x_{break}
3	R	0.150	0.166	193.8	0.079	0.092	62.4
3	B	0.151	0.167	188.6	0.080	0.093	39.6
5	R	0.111	0.140	198.6	0.069	0.084	108.2
5	B	0.112	0.141	184.8	0.070	0.085	91.8
7	R	0.099	0.133	199.8	0.061	0.080	138.4
7	B	0.100	0.134	183.2	0.062	0.081	132.6
8	R	0.095	0.136	196.2	0.058	0.077	156.6
8	B	0.096	0.137	184.4	0.059	0.078	131.4
10	R	0.088	0.140	199.8	0.054	0.072	199.0
10	B	0.089	0.141	192.0	0.055	0.073	178.8

For simplicity, both steepnesses use the same notation s_0. In each case and for each N, the value s_0 is the threshold value for recurrence (R) and breaking (B).

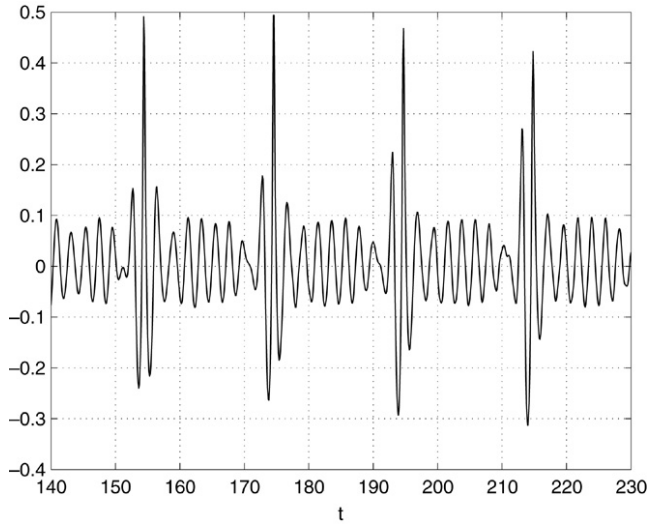

Fig. 2. Benjamin–Feir signal for $N = 5$ at x_{max}, the location where $\alpha(x) = \max_t \eta(x,t)$ achieves its maximum within the tank. Observe the large amplification: compared with the Benjamin–Feir signal generated at the wave maker, it can be seen that there is an amplification factor of ≈2.5.

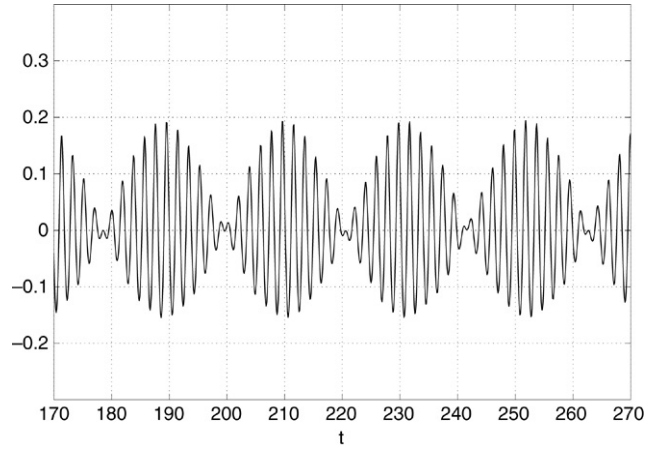

Fig. 3. Bichromatic signal for the case $N = 5$ at the wave maker. The period for the monochromatic wave is $T_{wave} \approx 1.9147$ s, while the period for the envelope is $T_{env} \approx 42.0280$ s. In the bichromatic case, one envelope makes two beats. In one signal beat, there are approximately ten monochromatic waves, while the corresponding spatial beat contains five waves.

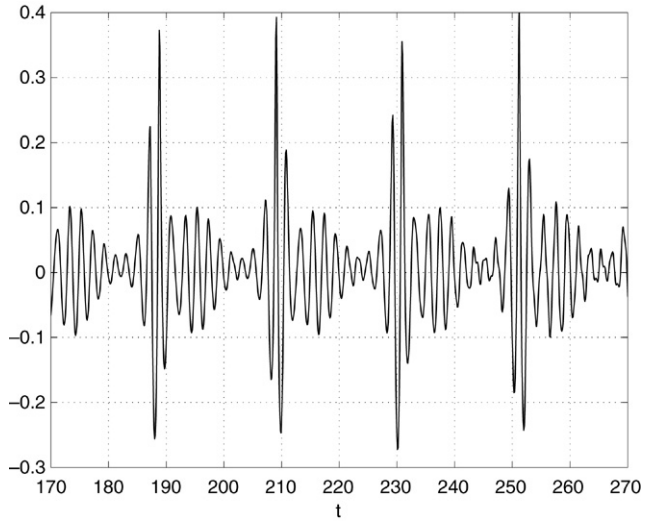

Fig. 4. The bichromatic signal for $N = 5$ at x_{max}, the location where $\alpha(x) = \max_t \eta(x,t)$ achieves its maximum within the tank. Comparing $\alpha(x_{max})$ and $\alpha(0)$ at the wave maker, we deduce that the amplification factor is approximately 2.

The threshold values of $s_0 = a_0 k_0$ for different values of N for both cases is presented in Fig. 5. For a given N, the threshold value of s_0 is the largest value of the initial wave steepness at the wave maker, so that the wave will not break during its propagation. It can be seen in this figure that the threshold values for the initial wave steepness at the wave maker for the bichromatic case are almost twice as large as the corresponding values for the BF case. The reason for this is because s_0 is defined as $a_0 k_0$. In the BF case, the amplitude of the envelope is $a_0 + 2\epsilon a_0$ for small ϵ, while in the bichromatic case this amplitude is $2a_0$. Thus it can be said that the actual initial wave steepness in the BF case is $(a_0 + 2\epsilon a_0)k_0$, while in the bichromatic case it is $2a_0 k_0$.

A comparison with experimental results is presented in Fig. 6 for bichromatic wave groups. Here, three pairs of experiments reported in [22] are compared with the numerical results. Each of the pairs describe non-breaking and breaking experiments based on the initial steepness of waves at the wave maker close to the threshold of breaking. The non-breaking wave in the first pair has a steepness slightly above the threshold

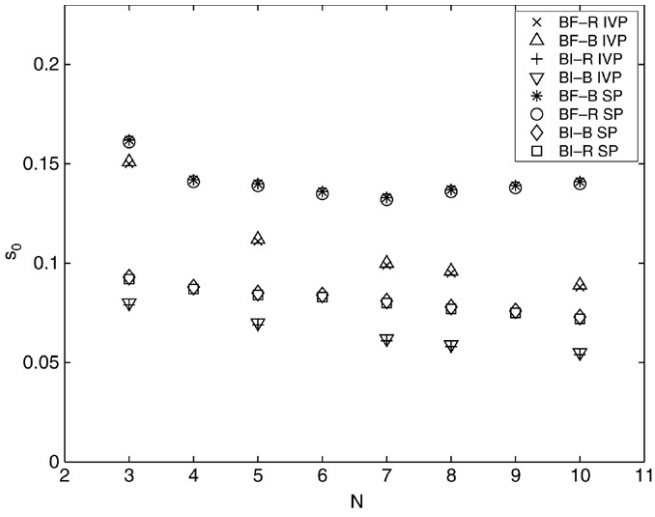

Fig. 5. The dependence of the initial wave steepness s_0, defined as a_0k_0, on the number of waves N for the Benjamin–Feir and bichromatic cases. For each N, this s_0 is the threshold value for recurrence and breaking patterns. BF-R and BF-B in the legend stand for Recurrence and Breaking for the Benjamin–Feir case, respectively. Similarly, Bi-R and Bi-B stand for Recurrence and Breaking for the bichromatic case, respectively. Here, s_0 for the bichromatic case is almost twice as large as that for the BF case. The amplitude of the envelope in the BF case is $a_0 + 2\epsilon a_0$ for small ϵ, while in the bichromatic case it is $2a_0$.

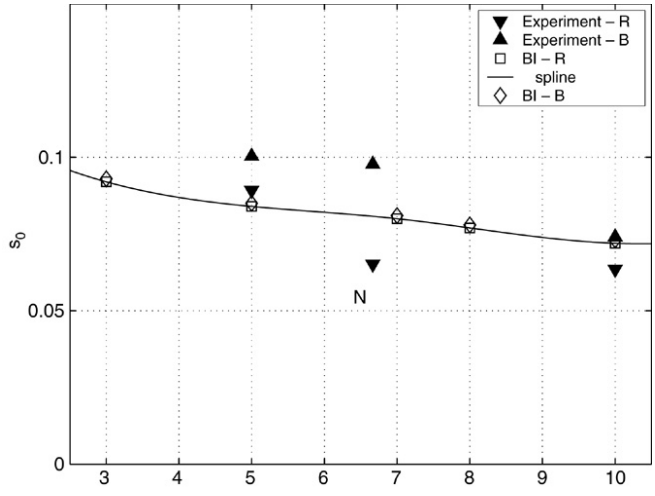

Fig. 6. A comparison between the numerical threshold values for recurrence and breaking patterns. Bi-R and Bi-B in the legend stand for Recurrence and Breaking for the bichromatic case, respectively. Three pairs of experiments are compared with the numerical threshold values. Experiment-R and Experiment-B in the legend stand for Breaking and Recurrence for the experiments, respectively. Except for the first pair of experiments, where Recurrence occurs slightly above the numerical threshold, this comparison indicates that the numerical threshold values for wave steepness can be used to guide the experiments.

of breaking predicted by the numerical calculation. In the second and third pairs of experiments, the initial steepness of the non-breaking waves are below the numerical threshold, while the the initial values of steepness of the breaking waves are located above it. These results show that the numerical thresholds of the initial values of steepness are reasonably good indicators for experiments.

From the results presented in Table 3, it becomes clear that the threshold value for the initial steepness is, in all cases considered, larger for the signaling problem than for the IVP. The signaling problem allows steeper initial waves that do not break during their evolution. Furthermore, for the IVP of BF and bichromatics, the maximum steepness s_0, below which no breaking occurs, decreasing as N increases. This is also true for our investigation of the signaling problem for the case of the bichromatic signals, but it is not true for the Benjamin–Feir case.

A rather large deviation from the remaining results for BF signals is observed for the case $N = 3$; see Table 3 and Fig. 5. For $N = 3$, BF theory may not be relevant, as investigated in [26]. Another explanation is as follows. It is known that there is an exact solution of the nonlinear Schrodinger (NLS) equation called Soliton on Finite Background (SFB), which is a nonlinear extension of the Benjamin–Feir instability. Besides SFB, actually, large-amplitude phenomena are also present in two different but closely related explicit solutions of the NLS: the class of Ma-solutions and the single polynomial solution of Peregrine; see [27–29]. Given the frequency ω_0 of the monochromatic background, SFB written in the field variables has two other parameters, namely the modulation frequency ν, that is, the frequency of the envelope of the wave group, and the amplitude of the monochromatic a_0 at infinity. The Benjamin–Feir instability region is $0 < \hat{\nu} < \sqrt{2}$, where $\hat{\nu} = \nu/\nu^*$ and $\nu^* = a_0 * \sqrt{\gamma/\beta}$. Here the parameters γ and β are the coefficients of nonlinearity and of dispersion respectively; these depend on ω_0 and appear in the spatial NLS equation as follows:

$$\frac{\partial A}{\partial \xi} + \mathrm{i}\beta \frac{\partial^2 A}{\partial \tau^2} + \mathrm{i}\gamma |A|^2 A = 0.$$

If the normalized modulation frequency $\hat{\nu}$ of the BF signal lies within the Benjamin–Feir instability region, this BF signal evolves according to the solution given by SFB, and hence it will show deformation and amplification. In particular, the largest amplifications appear in between phase singularities, i.e. the zeros of wave amplitude. Such singularities (associated with wave dislocations) happen for $0 < \hat{\nu} < \sqrt{3/2}$, and the most extreme waves are sandwiched between these singularities [30, 31]. For the case $N = 3$, the monochromatic frequency is $\omega_0 = 3.0865$, while the modulation frequency is $\nu = 0.5295$. The smallest value for the amplitude of the monochromatic a_0 such that $\hat{\nu}$ lies in the phase singularity region is $a_0^{\mathrm{crit}} \approx 0.1422$ m. It is likely that the threshold of breaking is for $a_0 > a_0^{\mathrm{crit}}$. We observe that a_0^{crit} for the case $N = 3$ is far above the values for larger $N = 5, 7, 8, 10$; see the list below.

N	3	5	7	8	10
a_0^{crit}	0.1422	0.0718	0.0588	0.0525	0.0410

3.2. Wave-breaking indicator for signaling problem

In [11], it is argued that the quantity $\mu(t)$ defined above in (1) and its evolution is an important indicator for the occurrence

Table 4
Initial time T_0 and t_{onset} used in the computation of $\bar{\delta}^{\max}$ for the signaling problems

N	R/B	Benjamin–Feir case				Bichromatics case			
		s_0	T_0	t_{br}	t_{ons}	s_0	T_0	t_{br}	t_{ons}
3	R	0.166	127.1	–	–	0.092	138.4	–	–
3	B	0.167	127.1	282.8	282.7	0.093	138.4	299.4	299.3
5	R	0.140	134.6	–	–	0.084	147.2	–	–
5	B	0.141	134.6	267.9	267.6	0.085	147.2	287.8	287.7
7	R	0.133	132.4	–	–	0.080	135.6	–	–
7	B	0.134	132.4	299.1	298.7	0.081	135.6	282.8	282.7
8	R	0.136	131.3	–	–	0.077	138.3	–	–
8	B	0.137	131.3	284.4	284.3	0.078	138.3	297.6	297.4
10	R	0.140	142.0	–	–	0.072	138.5	–	–
10	B	0.141	142.0	278.2	278.0	0.073	138.5	280.6	280.5

The values T_0 are such that, in all the generated data, the wave-breaking indicator is calculated over a time interval from $T_0 = t_0 + L/V_g$ to T_s.

of wave breaking in the case of waves evolving in time from a given wave field. Since our interest is in determining a parameter of wave breaking for waves generated at a wave maker and propagating in still water, we adjust this quantity. This leads to the definition of a space-dependent quantity that provides, at each position, the maximum over time of the squared steepness:

$$\breve{\mu}(x) = \max_t \left[\frac{E(x,t)}{\rho_w g} k^2(x,t) \right], \quad t \in [T_0, T_m],$$

where

$$T_m = \begin{cases} T_s & \text{in the case of recurrence} \\ t_{\text{onset}} & \text{in the case of breaking.} \end{cases}$$

Here, t_{onset} is a time chosen to be close to the time of breaking, t_{br}. The value of t_{br} is determined by the time of blow-up of the code. For each time t^* close before t_{br}, the function $\breve{\mu}(x)$ is still finite. Fast oscillations and large values of $\breve{\mu}(x)$ (details of which depend on t^*) indicate the position where the breaking will occur. It is important to note that the threshold values to be determined later are calculated only from non-breaking cases; for cases for which recurrence is observed. Hence the precise choices of the values t_{onset} have no effect on the threshold value. The meaning of this threshold value is explained in the next subsection. For the cases investigated here, BF and bichromatics, for each N, the times t_{onset} are listed in Table 4.

The calculation of the quantity $\breve{\mu}(x)$ for realistic wave fields can be rather complicated and time consuming, since it requires us, in principle, to determine the local wave number at each position. Hilbert transformation is often used to compute the local wave number, such as in [11]. To simplify the calculation, however, we use a somewhat different method based on the intuitive idea that at each position the maximal steepness can be expected to occur at the time of the largest wave. Then, at a given position, we first find the time at which the largest wave height is obtained, and then calculate the local wave number through zero crossing at that time only. So, if we denote this time by $t_{\max} = t_{\max}(x)$, we consider

$$\hat{\mu}(x) = \max_t \left[\frac{E(x,t)}{\rho_w g} \right] k^2(x, t_{\max}). \tag{5}$$

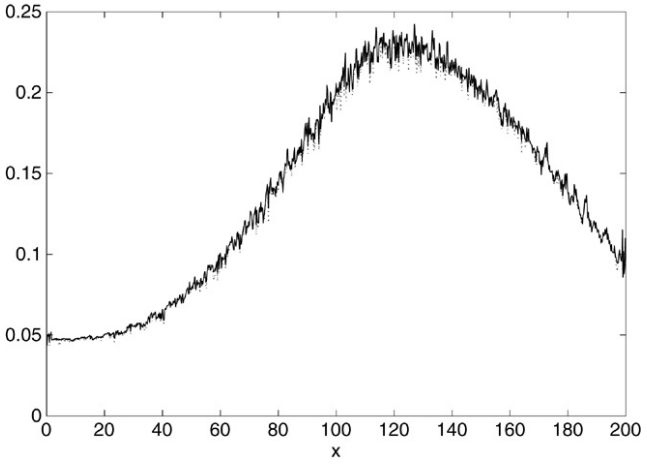

Fig. 7. Comparison between the maximal temporal steepness $\bar{\mu}(x)$ (grey, solid line) and the similar quantity $\hat{\mu}(x)$ (black, dotted line) with the local wave number computed at $t_{\max}$, the time for which the largest wave height is obtained. It shows here that the two quantities almost coincide at each position x.

Furthermore, it is found in the numerical results that $\max_t E(x,t)$ can well be approximated by $E(x, t_{\max})$. Thus, with this observation, the expression for $\breve{\mu}(x)$ will be further simplified to

$$\bar{\mu}(x) = \frac{E(x, t_{\max})}{\rho_w g} k^2(x, t_{\max}).$$

We refer to the last quantity $\bar{\mu}(x)$ as the *squared maximal temporal steepness*.

In Fig. 7, we show a comparison between $\hat{\mu}(x)$ and $\bar{\mu}(x)$ for the bichromatic case as an example with $\eta(0,t) = q\cos(\omega_1 t) + q\cos(\omega_2 t)$, with $q = 0.08, \omega_1 = 3.3$ and $\omega_2 = 2.99$. These plots show that the two quantities almost coincide at each position x. The oscillatory property of the quantities is caused by interactions between second-order bound waves and second-order free waves; the bound waves result from mode generation, while the free waves result from the wave-maker motion. As the input signals at the wave maker are correct up to the second orders, these second harmonics are generated during the wave group evolution. This oscillating behaviour has been calculated with an expansion method; see [25].

Besides $\bar{\mu}(x)$ defined above, we consider the *spatial variation* of the *squared maximal temporal steepness*,

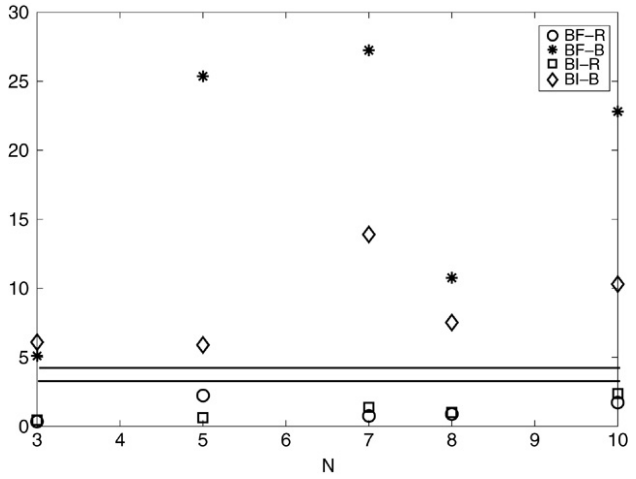

Fig. 8. Values of $\bar{\delta}^{\max}$ for Benjamin–Feir and bichromatic cases. For the case of breaking, computations for $\bar{\delta}^{\max}$ are performed using the wave fields in the interval $[T_0, t_{\text{onset}}]$. The graph indicates the existence of thresholds for the values $\bar{\delta}^{\max}$ below which no breaking can occur for the two cases considered here.

$$\bar{\delta}(x) = \frac{1}{k_0}\frac{\mathrm{d}}{\mathrm{d}x}\bar{\mu}(x), \tag{6}$$

where k_0 is the wave number of the initial wave. We note here that the computation of $\bar{\delta}(x)$ does not use any smoothing, which is different from considering the averaged value $\langle\bar{\mu}(x)\rangle$ as is done in [11]. The resulting $\bar{\delta}(x)$ is of course larger than if smoothing and averaging is used; this $\bar{\delta}(x)$ captures locally the oscillatory character of $\bar{\mu}(x)$.

Now the global quantity $\max_x \bar{\delta}(x)$ will be used as the wave-breaking criterion for the signaling problem in the next subsection.

3.3. Wave-breaking criterion for signaling problem

In [11], for the case of a recurrent pattern, $\delta^{\max}$ is defined to be $\max_t \delta(t)$, and then the corresponding t that produces this $\delta^{\max}$ is denoted by $t_{\max}$. For the breaking case, $\delta^{\max}$ is defined to be $\delta(t_{\text{break}})$, where t_{break} is the time that signifies the onset of breaking. For the signaling problem that we study here, we define analogously

$$\bar{\delta}^{\max} = \begin{cases} \max\limits_x \bar{\delta}(x); & \text{in the case of recurrence} \\ \bar{\delta}(x_{\text{break}}); & \text{in the case of breaking.} \end{cases}$$

Here, x_{break} is the location where the signal start to break within the towing tank.

In Fig. 8, we plot $\bar{\delta}^{\max}$ for the cases considered above. Just as for the IVP for the evolution of ocean waves presented in [11], we observe that for BF and bichromatic wave fields it is possible to define a threshold value below which no breaking occurs. This threshold value is only determined by the recurrence cases for both BF and bichromatic wave fields. In the plot, this is indicated by the band near the value of 4.

The meaning of this threshold value is that, if at any position L the quantity $\bar{\delta}(L)$ measured in time $[0, T]$ is larger than the threshold value 4, then this wave train will break after some time $t > T$ at some location in the wave tank.

We note that the parameter $\bar{\delta}(x = 0)$ at the position of the wave maker, however, is not a predictive quantity for the cases studied here.

3.4. Relation between breaking criterion for IVP and signaling problems

It can be expected that there is a relation between the quantity $\delta(t)$ used in [11] and $\bar{\delta}(x)$ as defined above. We will derive this relation here.

Writing the squared local steepness as $S(x,t) = \frac{E(x,t)}{\rho_w g}k^2(x,t)$, we can write approximately $\delta(t) = \frac{1}{\omega_0}\frac{\mathrm{D}\mu(t)}{\mathrm{D}t}$, where $\mu(t) = \max_x S(x,t) = S(x_{\max}(t), t)$ and so $\delta(t) = \frac{1}{\omega_0}\{\frac{\partial S}{\partial t} + \frac{\partial S}{\partial x}\frac{\partial x_{\max}(t)}{\partial t}\}$. As described above, $\bar{\mu}(x) = \max_t S(x,t) = S(x, t_{\max}(x))$ and so $\bar{\delta}(x) = \frac{1}{k_0}\frac{\mathrm{d}}{\mathrm{d}x}S(x, t_{\max}(x)) = \frac{1}{k_0}\{\frac{\partial S}{\partial x} + \frac{\partial S}{\partial t}\frac{\partial t_{\max}}{\partial x}\}$. Intuitively, one expects, and this has been confirmed by numerical calculations that we have investigated, that $\frac{\partial x_{\max}(t)}{\partial t} = V_g$ while $\frac{\partial t_{\max}(x)}{\partial x} = 1/V_g$, where V_g is the wave group velocity. Using these results, we find that

$$\delta(t) = \frac{V_g}{\omega}\left\{\frac{1}{V_g}\frac{\partial S}{\partial t} + \frac{\partial S}{\partial x}\right\} = \frac{V_g}{\omega_0/k_0}\bar{\delta}(x) = \frac{V_g}{V_{ph}}\bar{\delta}(x),$$

where V_{ph} is the phase velocity of individual waves. With this reasoning, it is clear that if $\max_t \delta(t)$ can be used as breaking criteria for ocean waves, then $\max_x \bar{\delta}(x)$ is the natural quantity for the corresponding signaling problem.

4. Concluding remarks

We have considered two classes of wave groups, namely Benjamin–Feir (BF) and bichromatics, generated at a wave maker and running in still water. The propagation is investigated to see if breaking occurs and, if so, at which position in the tank. For several cases in each class, we have first investigated the breaking and the recurrence pattern as a function of the initial wave steepness at the wave maker. We have compared the numerical threshold values of this initial steepness for breaking with that of experimental results. We have defined a breaking criterion which is adjusted, but similar, to a corresponding quantity proposed by Song and Banner for the evolution of ocean waves from given initial profiles. In the signaling problems investigated here, at each position in the wave tank the breaking criterion $\bar{\delta}(x)$ measures the spatial variation of the maximum over time of the squared steepness. For the two cases considered, this breaking criterion $\bar{\delta}(x)$ is a predictive quantity for the onset of breaking within the wave tank.

A comparison of results between the signaling problems and the initial value problems shows that the maximal initial steepness without breaking can be more extreme in the signaling case than in the case of the initial value problem. Except for some non-monotonic detailed behaviour for the Benjamin–Feir case, results for the initial parameters obtained here are similar to the results obtained in [11] for the evolution of ocean waves from given initial wave fields. In this signaling problem, the initial steepness parameter refers to the value of the parameter at the wave maker, while in [11] it is for the value at the initial time.

Further, we observed that, for the two cases studied here, for waves propagating in still water there is a threshold, say Δ, for the breaking quantity $\bar{\delta}(x)$ below which no breaking occurs: given some position, say $x = L$, if during any interval of observation $[0, T]$, it holds that $\bar{\delta}(L) > \Delta$, then this wave train will break after some time $t > T$ at some location in the wave tank. Although this threshold value Δ is computed only for the two cases, it is likely also to be relevant for other wave trains; further studies will have to confirm this. The parameter $\bar{\delta}(x = 0)$ evaluated at the position of the wave maker, however, is not a predictive quantity for the cases studied here.

Acknowledgements

The authors are very grateful to Ir. Gert Klopman and Dr. Rene Huijsmans for fruitful discussions throughout the execution of this research. They would like to thank to Dr. Jaap-Harm Westhuis for the use of the numerical HUBRIS code. They greatly appreciate the help of Professor M.L. Banner for many references on the subject sent to us. They greatly thank the referee for the very careful and detailed comments that led to a very significant improvement of the original manuscript. This research is conducted partly at Institut Teknologi Bandung, Indonesia and partly at the University of Twente, The Netherlands and is supported by Riset Unggulan Terpadu Internasional (RUTI 2002/2005) in a collaboration with the University of Twente, STW project TWI5734 and by the Scientific Programme Indonesia Netherlands, Extended Programme in Applied Mathematics.

References

[1] Dean RG. Water wave kinematics. Amsterdam: Kluwer; 1990. p. 609–12.
[2] Longuet-Higgins MS. Statistical properties of wave groups in a random sea state. Philos Trans Roy Soc London 1984;A312:219–50.
[3] Phillips OM, Gu D, Donelan MA. Expected structure of extreme waves in a Gaussian sea. Part I. Theory and SWADE buoy measurements. J Phys Oceanogr 1993;23:992–1000.
[4] Donelan MA, Hui WH. Mechanics of ocean surface waves. In: Geernaert GL, Plants WJ, editors. Surface Waves and Fluxes, vol. 1. Kluwer; 1990. p. 209–46.
[5] Henderson KL, Peregrine DH, Dold JW. Unsteady water wave modulation: fully nonlinear solutions and comparison with the nonlinear Schroedinger equation. Wave Motion 1999;341.
[6] Dysthe K. Note on a modification to the nonlinear Schroedinger equation for application to deep water waves. Proc R Soc London, Ser A 1979;369: 105.
[7] Benjamin TB, Feir JE. The disintegration of wave trains on deep water. Part 1. Theory J Fluid Mech 1967;27:417.
[8] Holthuijsen LH, Herbers THC. Statistics of breaking waves observed as whitecaps in the open sea. J Phys Oceanogr 1986;16:290–7.
[9] Osborne AR, Onorato M, Serio M. The nonlinear dynamics of rogue waves and holes in deep-water gravity wave trains. Phys Lett 2000;A275: 386–93.
[10] Onorato M, Osborne AR, Serio M, Bertone S. Freak waves in random oceanic sea states. Phys Rev Lett 2001;86:5831.
[11] Song J-B, Banner ML. On determining the onset and strength of breaking for deep water waves, Part 1: Unforced irrotational wave groups. J Phys Oceanogr 2002;32:2541–58.
[12] Banner ML, Tian X. On the determination of the onset of wave breaking for modulating surface grafity water waves. J Fluid Mech 1998;367: 107–37.
[13] Griffin OM, et al. Kinematic and dynamic evolution of deep water breaking waves. J Geophys Res 1996;101(C7):16515–31.
[14] Melville WK. The instability and breaking of deep-water wave. J Fluid Mech 1982;115:165–85.
[15] Tulin MP, Li J. On the breaking of energetic waves. Int J Offshore Polar Eng 1992;2:46–53.
[16] Rapp RJ, Melville WK. Laboratory measurements of deep water breaking waves. Philos Trans Roy Soc London 1990;A331:735–800.
[17] Kway JHL, Loh YS, Chan ES. Laboratory study of deep water breaking waves. Ocean Eng 1998;25:657–76.
[18] Dold JW, Peregrine DH. Water-wave modulation. In: Proc. 20th int. conf. on coastal engineering. ASCE; 1986. p. 163–75.
[19] Westhuis JH. The numerical simulation of nonlinear waves in a hydrodynamic model test basin. Ph.D. thesis. The Netherlands: University of Twente; 2001. http://www.math.utwente.nl/aamp/FormMem/Westhuis/.
[20] van Groesen EWC, Westhuis JH. Modelling and simulation of surface water waves. Math Comput Simul 2002;59(4):341–60.
[21] Westhuis JH, Andonowati. Applying the finite element method in numerically solving the two dimensional free-surface water wave equations. In: Hermans AJ, editor. The 13th international workshop on water waves and floating bodies. The Netherlands: Alphen a/d Rijn; 1998. p. 171–4.
[22] Westhuis JH, van Groesen E, Huijsmans RHM. Long time evolution of unstable bichromatic waves. In: Miloh T, editor. The 15th international workshop on water waves and floating bodies. 2000. p. 184–7.
[23] Westhuis JH, van Groesen E, Huijsmans RHM. Experiments and numerics of bichromatic wave groups. J Waterway, Port, Coastal Ocean Eng 2001; 127:334–42.
[24] Westhuis JH. Approximate analytic solutions and numerical wave tank results for the reflection coefficients of a class of numerical beaches. In: Proceedings of the 10th ISOPE conference, vol. 3. 2000. p. 242–52.
[25] Andonowati, van Groesen E. Optical pulse deformation in second order non-linear media. J Nonlinear Optical Phys Mater 2003;12:221–34.
[26] Longuet-Higgins. The instability of gravity waves of finite amplitude in deep water, II. Subharmonic, Proc Roy Soc A 1978;360:489–505.
[27] Akhmediev NN, Ankiewicz A. Solitons, nonlinear pulses and beams. London: Chapman & Hall; 1997.
[28] Ma Y-C. The perturbed plane-wave solutions of the cubic Schrödinger equation. Stud Appl Math 1979;60:43–58.
[29] Peregrine DH. Water waves, nonlinear Schrödinger equations and their solutions. J Austr Math Soc Ser B 1983;25:16–43.
[30] van Groesen E, Andonowati, Karjanto N. Displaced phase-amplitude variables for waves on finite background. Phys Lett A 2006;354:312–9.
[31] Andonowati, van Groesen E, Karjanto N. Extreme wave phenomena in down-stream running modulated waves. Appl Math Modelling 2006 [in press] (article can be downloaded from www.labmath-indonesia.or.id/Reports/Reports.htm).